

Electronic Supplementary Information (ESI)

**Surface-Oxidized Carbon Black is Catalysts for Water Oxidation and
Alcohol Oxidation Reactions**

Bryan H. R. Suryanto and Chuan Zhao*

School of Chemistry, The University of New South Wales, Kensington, NSW, 2052,
Australia.

Contents

1. Experimental section	S2
2. Particle size distribution analysis of r-CB.....	S4
3. X-ray diffraction	S5
4. Electrochemical activation process	S6
5. X-ray photoelectron spectroscopy for detecting metal impurities	S7
6. Visual detection of gas bubbles on the surface of working electrode	S8
7. Rotating ring-disk measurement (RRDE)	S9
8. Table of WOR catalysts performance	S10
9. Electrochemical performance of o-CB in 1 M KOH	S11
10. Determination of electrochemically active surface area (ECSA) measurement.....	S12
11. Electrochemical impedance spectroscopy	S14
12. Particle size distribution analyses of eco-CB and o-CB	S15
13. TEM micrographs of eco-CB and o-CB	S16
14. ECSA normalised cyclic voltammetry for WOR of eco-CB in 0.1 M KOH.....	S17
15. Table of XPS elemental composition.....	S18

1. Experimental section

Treatment of carbon black. High purity carbon black c-nergy super C65 (< 2 ppm metal impurities) was purchased from Timcal Ltd., Switzerland. Oxidized carbon black (o-CB) was prepared by subjecting 100 mg of r-CB into ultrasonication in 75 ml of 98% H₂SO₄ in a round bottomed flask for 20 min. The homogenous r-CB-H₂SO₄ suspension was magnetically stirred and 25 ml of 30% of H₂O₂ was cautiously added to prevent overheating of mixture. The mixture was continuously stirred for 4 hours in the 3:1 piranha mixture (H₂SO₄:H₂O₂). The acid oxidation process was then quenched using equal volume of Milli-Q water and the resultant o-CB was separated from the mixture by centrifugation at 5000 r.p.m. Oxidized carbon black were collected by centrifugation at 7000 r.p.m., rinsed thoroughly with Milli-Q water and dried in a vacuum oven at 40 °C overnight. For thermally reduced carbon black (t-CB), thermal reduction of o-CB was performed by annealing 50 mg of o-CB in a tube furnace, the temperature was ramped at rate of 5 °C min⁻¹ to 800 °C and the temperature was held for 1 h, annealing was performed under N₂ gas protection.

Electrochemical analysis. All voltammetries were collected using CHI 760 Electrochemical workstation using a glassy carbon rotating disk electrode (RDE), Ag/AgCl (1 M KCl) reference electrode and platinum wire as counter electrode. All the electrolytes were prepared using analytical grade KOH (Sigma-Aldrich) and Milli-Q water. The catalyst was loaded to the surface of electrode by initially preparing CB ink by ultrasonically 5 mg of the respective CB powder in 1 ml of 50% EtOH solution containing 20 µl of Nafion (5 wt.%, Sigma-Aldrich) for 20 min until homogenous mixture was obtained. Six microliters of the ink were then drop-casted to the surface of the RDE/RRDE disk-electrode with surface area of 0.12 cm² and air-dried to achieve a smooth layer of the catalyst. All experiments were

carried out in 0.1 M KOH electrolytes with a typical scan rate of 5 mV s⁻¹ and 1600 r.p.m. rotation, unless otherwise stated. For comparison, potentials reported in this study was reported in E_{RHE} (against reversible hydrogen electrode) using the equation $E_{RHE} = E_{Ag/AgCl} (1 \text{ M KCl}) + 0.235 \text{ V} + 0.059 \text{ pH}$. Unless specifically mentioned the polarization curves shown in this work are the second-sweep as the initial sweeps do not represent actual electrochemical response and often contains large residual currents as well as large capacitance currents.

Physical characterizations. Scanning electron microscopy (SEM) images was generated from FEI Nova NanoSEM 230 at 5.0 kV. Samples were prepared by adding the sample powders to the surface of carbon conducting tape. Transmission electron microscopy (TEM) images were performed using Phillips CM 200 at 200 kV with samples prepared by drop casting homogenous solution of CB in absolute ethanol to the surface of formvar coated copper grid. X-ray photoelectron spectroscopy (XPS) analyses were conducted using Thermo ESCALAB250i X-ray Photoelectron Spectrometer. Particle size measurements were generated by ImageJ software and the Gaussian peak fit was performed using Origin 8 data processor.

2. Particle size distribution analysis of r-CB

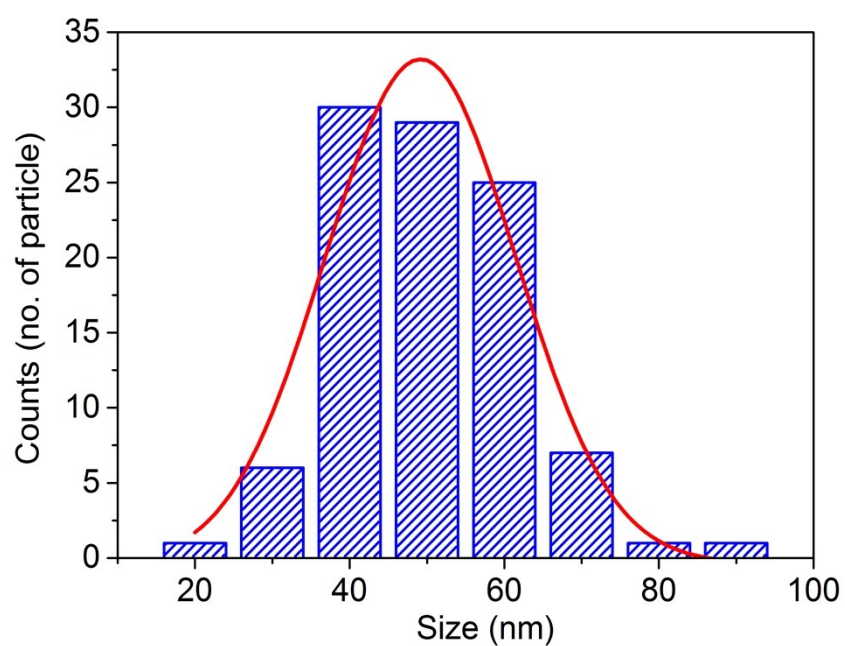


Figure S1. CB particle diameter distribution taken from 100 r-CB particles, the average size is 50 nm as shown by the Gaussian fit peak.

3. X-ray diffraction pattern

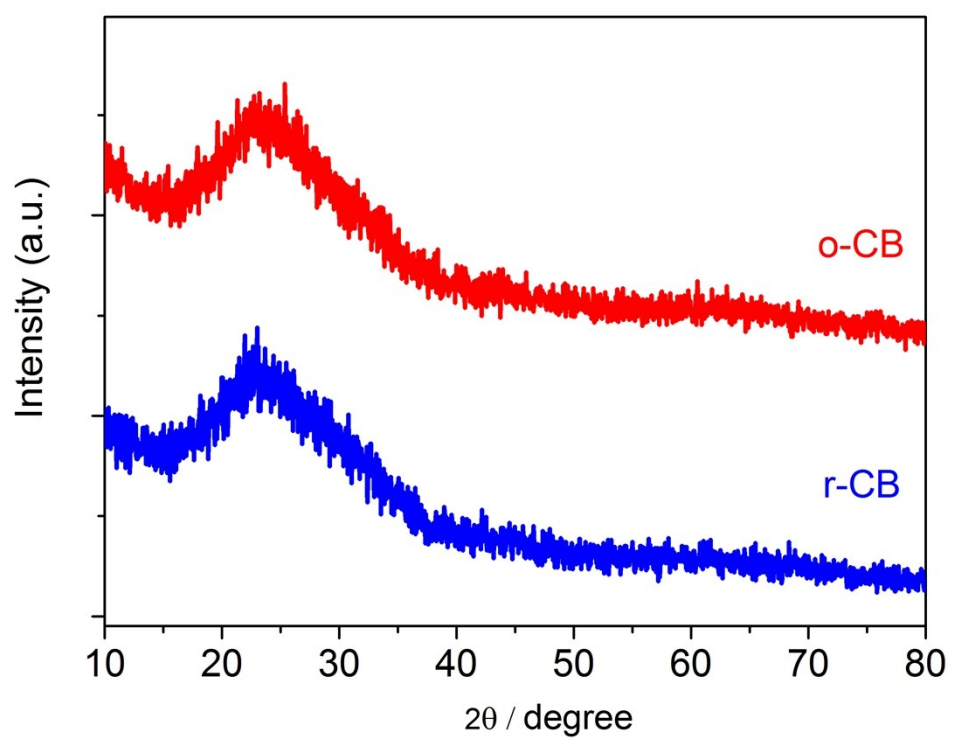


Figure S2. X-ray diffraction pattern obtained from o-CB and r-CB.

4. Electrochemical activation process

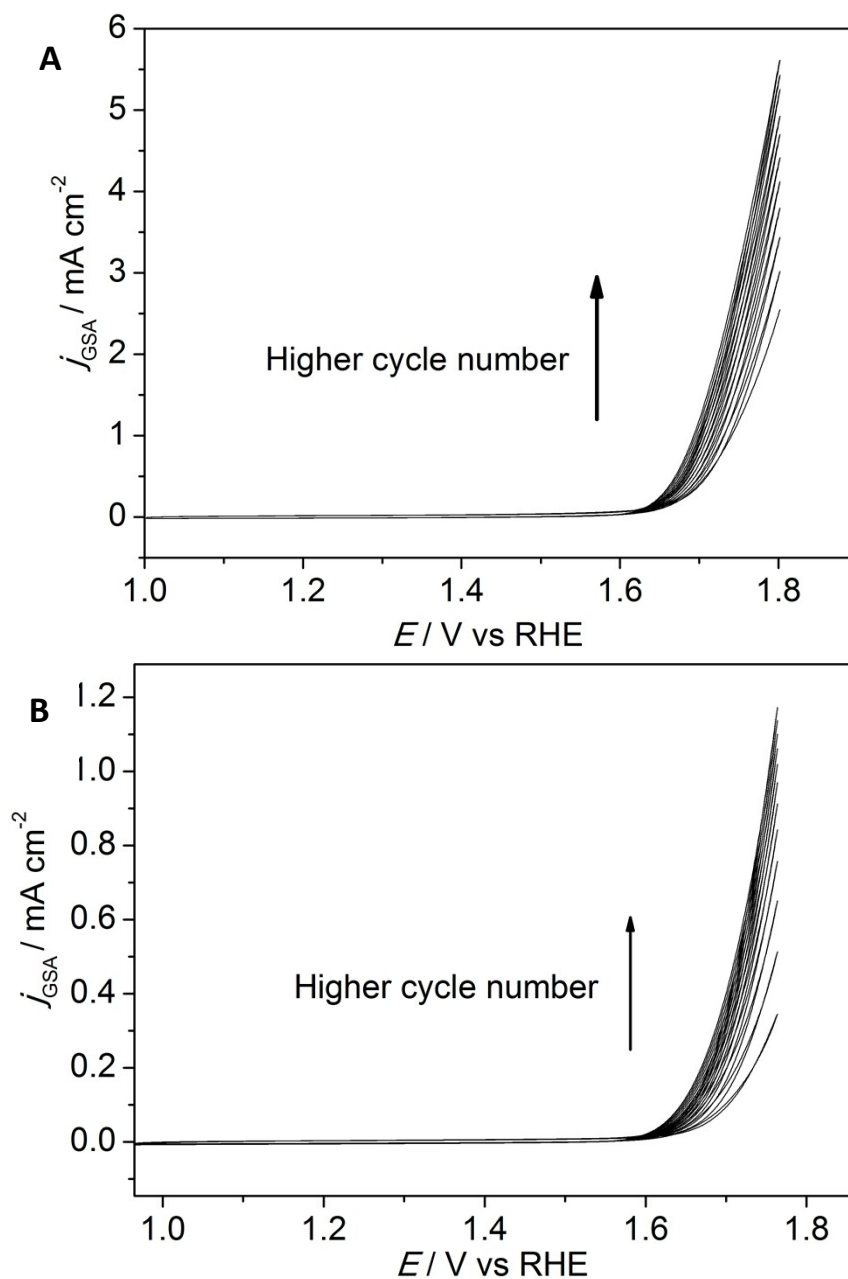


Figure S3. Cyclic voltammetry showing the electrochemical activation step performed on (A) o-CB and (B) r-CB in 0.1 M KOH collected with scan rate of 5 mV s^{-1} .

5. X-ray photoelectron spectroscopy for detecting metal impurities

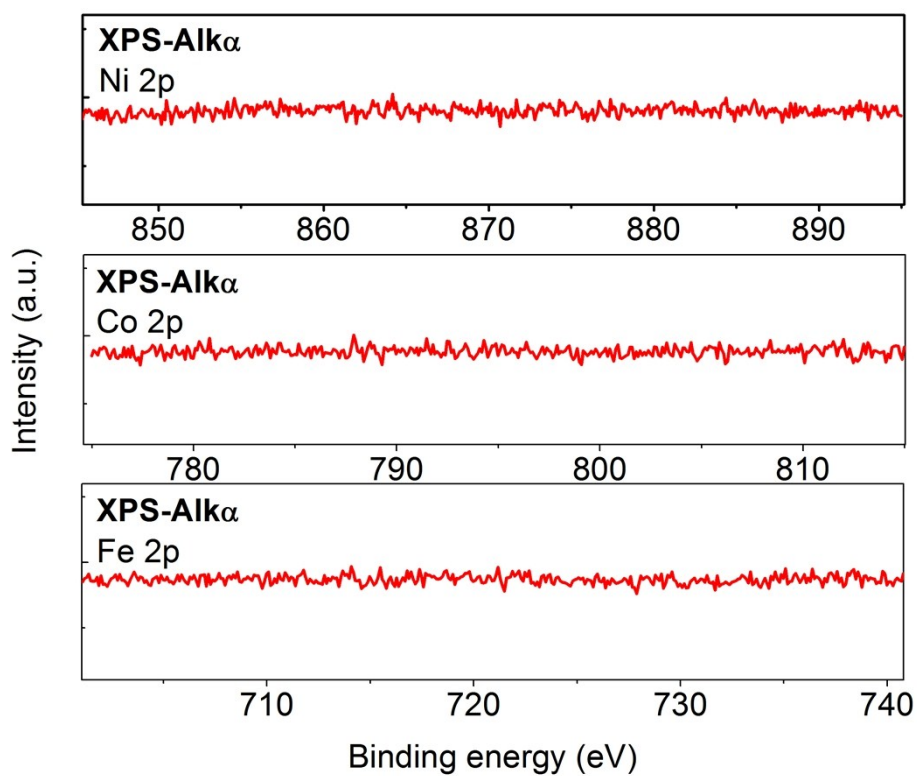


Figure S4. The high resolution XPS spectra of eco-CB for Ni 2p, Co 2p and Fe 2p regions.

6. Visual detection of



gas bubbles on the

surface of working electrode

Figure S5. The image of working electrode loaded with o-CB being polarized at 1.8 V at RHE. The image indicates the formation of gaseous bubbles during anodic polarization in 0.1 M KOH.

7. Rotating ring-disk measurement (RRDE)

Rotating ring disk measurement was done using Pt-ring glassy carbon disk electrode (ALS Co. Ltd.) as represented in the. Carbon black ink was drop-casted to the surface of disk electrode and dried under vacuum to afford homogenous cast. The potential of Pt-ring was set at 0.5 V vs. RHE to detect oxygen generated at OER by the way of oxygen reduction reaction (ORR). The Faradaic efficiency of the reaction was determined using the following equation:

$$\text{Faradaic efficiency} = \frac{j_{ORR}}{j_{OER} \times N} \times 100\% \quad (4)$$

Where N is the collection efficiency ($N = 0.424$) according to manufacturer data sheet, $j_{ORR/OER}$ are the current density of OER/ORR collected from GC disk electrode and Pt-ring electrode. During the measurement the rotating speed was set at 1600 r.p.m.

8. Table of WOR catalysts performances

Table S1. Comparison of WOR electrocatalysts performances.

Carbon Catalyst	Electrolyte (KOH)	Dopant	Overpotential (η) @ 10 mA cm⁻¹	References
eco-CB	0.1 M	O	620 mV	This work
	1.0 M	O	440 mV	This work

echo-CNT	0.1 M	O	360 mV	<i>J. Am. Chem. Soc.</i> 2015 , 137, 2901-2907.
O-CC	0.1 M	O	477 mV	<i>Chem. Comm.</i> , 2015 , 51, 1616-1619.
CcNT-ACN	0.1 M	N	450 mV	<i>ACS Appl. Mater Interfaces.</i> 2015 , 7, 11991-12000.
CCNT-DMF	0.1 M	N	470 mV	<i>ACS Appl. Mater Interfaces.</i> 2015 , 7, 11991-12000.
C ₃ N ₄ - GR	0.1 M	N	539 mV	<i>ChemSusChem</i> , 2014 , 7, 2152-2132.
NG-CNT	0.1 M	N,O	534 mV	<i>Adv. Mater.</i> , 2014 , 26, 2925-2930.
N-C	0.1 M	N, Ni trace	380 mV	<i>Nat. Comm.</i> , 2013 , 4:2390.
Metal Catalysts				
MnOx	1.0 M	N/A	540 mV	<i>J. Am. Chem. Soc.</i> 2010 , 132, 13612
Co ₃ O ₄	1.0 M	N/A	328 mV	<i>J. Phys. Chem. C</i> 2009 , 113, 15068.
20% Ru/C	0.1 M	N/A	390 mV	<i>J. Am. Chem. Soc.</i> 2010 , 132, 13612
20% Ir/C	0.1 M	N/A	380 mV	<i>J. Am. Chem. Soc.</i> 2010 , 132, 13612

9. Electrochemical performance of o-CB in 1 M KOH

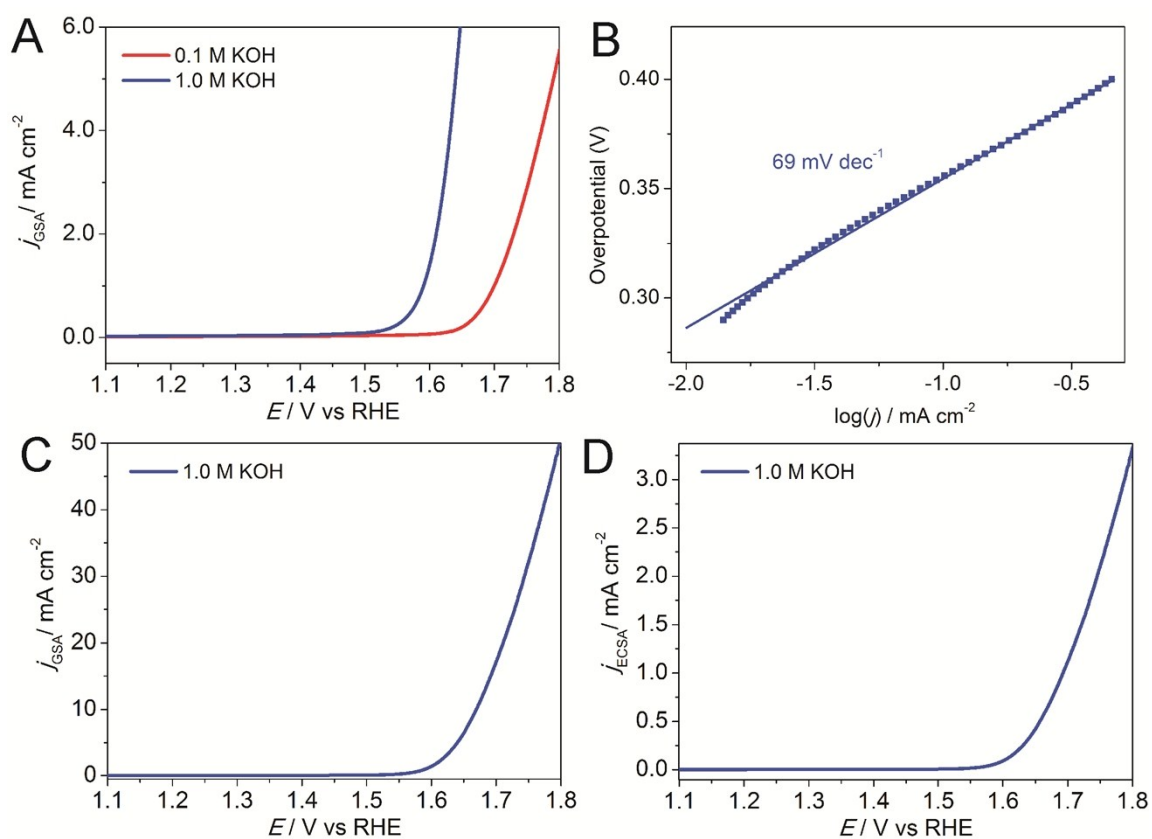


Figure S6. LSVs of eco-CB collected in both 0.1 M and 1 M KOH; (B) Tafel slope of eco-CB, (C) LSV of eco-CB (high current density), (D) LSV of eco-CB (ECSA current density). The voltammetric measurements in (B-D) were all collected in 1 M KOH with iR -compensation and at a scan rate of 5 mV s^{-1} .

10. Determination of electrochemically active surface area (ECSA) measurement

The measurement of ECSA was performed according to the previous study.¹ ECSA measurement is based on the double layer capacitance on the materials measured on glassy carbon RDE in 0.1 M KOH. Capacitance was measured by recording anodic-cathodic charging currents (i_c) in the potential region where Faradaic process is absent. The charging currents were collected at different scan rate (ν), hence double layer capacitance can be calculated according to eq. 1

$$i_c = \nu C_{DL} \quad (1)$$

Therefore the plot of i_c vs ν will form a linear plot (Fig S2d) and the slope is equal to C_{DL} . The C_{DL} of o-CB and eco-CB measured according to the plot is 40.9 and 50.6 μF , respectively. The measurement of ECSA can be performed according to the following eq. 2

$$\text{ECSA} = \frac{C_{DL}}{C_s} \quad (2)$$

Specific capacitance (C_s) for carbon black value was reported previously to be $C_s = 27.50 \mu\text{F cm}^{-2}$.² Therefore, the calculated ECSA is 1.49 and 1.84 cm^2 for o-CB and eco-CB, respectively.

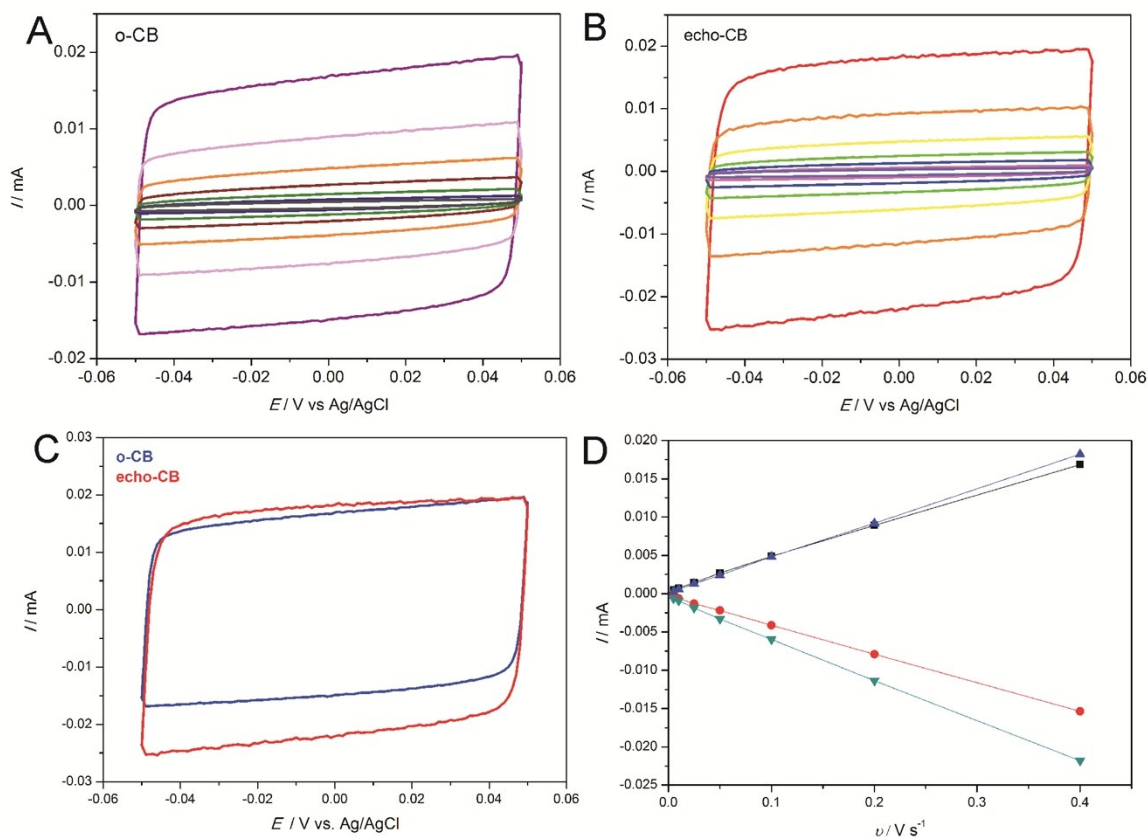


Figure S7. (a) Cyclic voltammograms obtained with o-CB and (b) eco-CB, by loading CB materials loaded on the glassy carbon electrodes in the capacitance current range (-0.05 V to 0.05 V vs Ag/AgCl) with scan rates of 5, 10, 25, 100, 200 and 400 mV. (c) Comparison between cyclic voltammograms between o-CB and eco-CB and (d) The cathodic and anodic charging current plot (i_c) vs scan rate (ν), the double layer capacitance value was determined by taking average of the absolute value of both anodic and cathodic slopes.

11. Electrochemical impedance spectroscopy

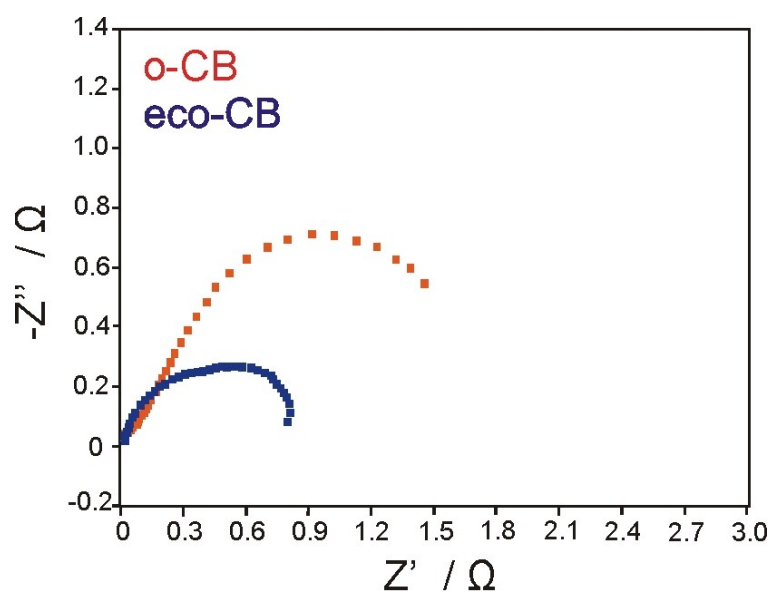


Figure S8. The Nyquist plot from electrochemical impedance spectroscopy measurements of o-CB and eco-CB

12. Particle size distribution analyses

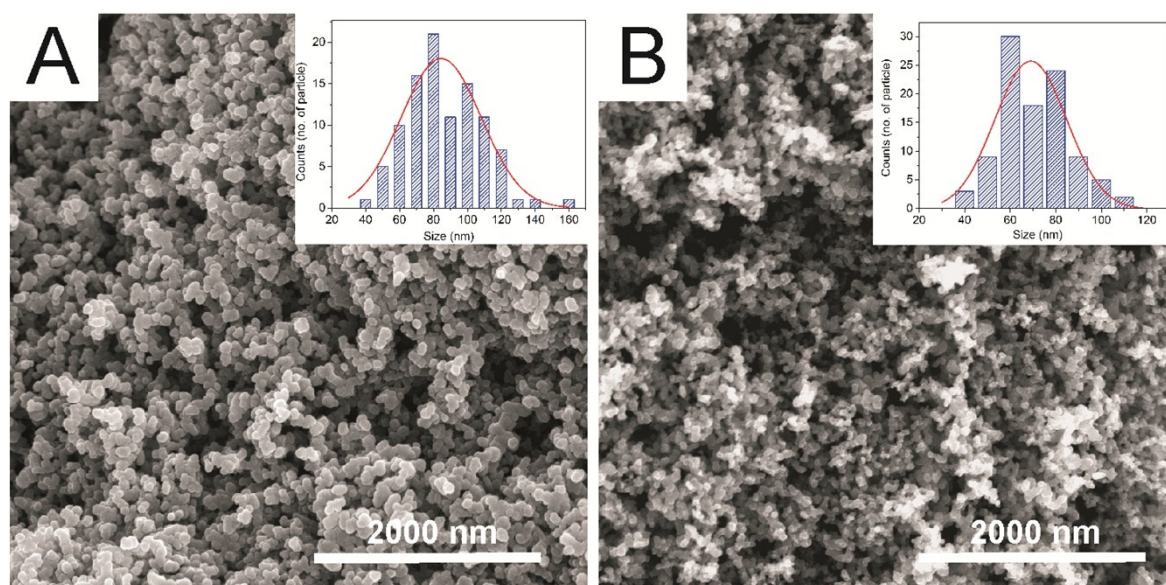


Figure S9. The SEM micrograph and the diameter distribution histogram of (A) eco-CB and (B) o-CB.

13. TEM micrographs of eco-CB and o-CB

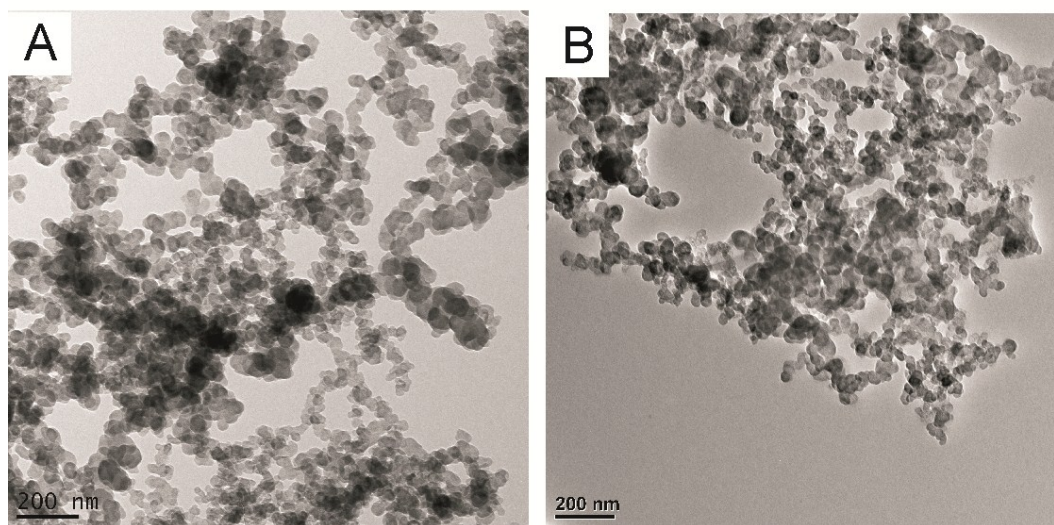


Figure S10. The TEM micrograph of (A) eco-CB and (B) o-CB.

14. ECSA normalised cyclic voltammetry for WOR of eco-CB in 0.1 M KOH

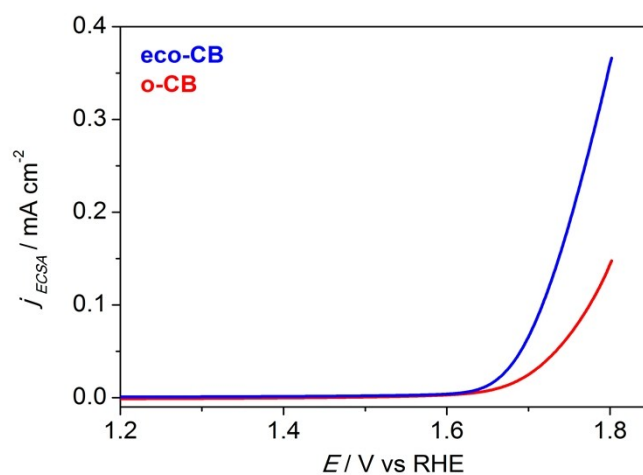


Figure S11. LSVs of eco-CB and o-CB for WOR in 0.1 M KOH, with current density normalised to their respective ECSA. LSVs were recorded at a scan rate of 5 mV s^{-1} .

15. Table of XPS elemental composition

Table S2. XPS elemental analysis of the carbon black samples

Sample Name	Ketonic (531.25 eV, at. %)	Hydroxyl (533.3 eV, at. %)	O (at. %)	Fe (at. %)	Ni (at.%)	Co (at.%)
r-CB	0.24	0.19	0.43	N.D.	N.D.	N.D.
o-CB	1.72	1.72	3.44	N.D.	N.D.	N.D.
t-CB	0.09	0.18	0.27	N.D.	N.D.	N.D.
eco-CB	5.1	2.81	8.87	N.D.	N.D.	N.D.

*N.D – not detectable

References:

1. McCrory CCL, Jung SH, Peters JC, Jaramillo TF. *J. Am. Chem. Soc.* 2013, **135**(45): 16977-16987.
2. Solorza-Feria O, Ramirez-Raya S, Rivera-Noriega R, Ordonez-Regil E, *Thin Solid Films* 1997, **311**(1-2): 164-170.